Journal of Structural Biology 183 (2013) 412–418

Contents lists available at SciVerse ScienceDirect

Journal of Structural Biology

journal homepage: www.elsevier.com/locate/yjsbi

High-resolution scanning electron microscopy of the cytoskeleton of *Tritrichomonas foetus*

Ivone de Andrade Rosa [a,b], Wanderley de Souza [c,d,e], Marlene Benchimol [a,d,*]

[a] *Universidade Santa Úrsula, Rio de Janeiro, Brazil*
[b] *Instituto de Biofísica Carlos Chagas Filho, Universidade Federal do Rio de Janeiro, Brazil*
[c] *Laboratório de Ultraestrutura Celular Hertha Meyer, Universidade Federal do Rio de Janeiro, Brazil*
[d] *Instituto Nacional de Ciência e Tecnologia em Biologia Estrutural e Bioimagens, Universidade Federal do Rio de Janeiro, Rio de Janeiro, Brazil*
[e] *Instituto Nacional de Metrologia, Qualidade e Tecnologia – Inmetro, Duque de Caxias, Rio de Janeiro, Brazil*

ARTICLE INFO

Article history:
Received 7 April 2013
Received in revised form 13 June 2013
Accepted 3 July 2013
Available online 15 July 2013

Keywords:
Tritrichomonas foetus
Cytoskeleton
Mastigont system
Pelta-axostyle system
Costa
Extreme high-resolution scanning electron microscopy

ABSTRACT

Tritrichomonas foetus is a pathogenic protozoan that causes bovine trichomoniasis. In addition to its importance in veterinary medicine, this parasite is also a good representative of one the earliest eukaryotic cells available for study. *T. foetus* contains organelles that are common to all eukaryotic cells as well as uncommon cell structures such as hydrogenosomes and a complex and elaborate cytoskeleton that constitutes the mastigont system. The mastigont system is mainly formed by several proteinaceous structures that are associated with basal bodies, the pelta-axostylar complex and the costa. Although the structural organization of trichomonad cytoskeletons has been analyzed using several techniques, observation using a new generation of scanning electron microscopes with a resolution of 0.8 nm has allowed more detailed visualization of the three-dimensional organization of the mastigont system. Moreover, this study revealed the presence of new structures, such as the costa accessory filament, and the presence of two groups of microtubules that form the pelta-axostylar system.

1. Introduction

Tritrichomonas foetus is a pathogenic protozoan that causes bovine trichomoniasis, one of the most widespread sexually transmitted diseases in cattle, which causes infertility and abortion and leads to considerable economic losses in beef-producing areas around the world (Rae and Crews, 2006). Furthermore, *T. foetus* is able to infect and colonize the colon of domestic cats, resulting in chronic, large-bowel diarrhea (Gookin et al., 2004; Stockdale et al., 2009; Yaeger and Gookin, 2005). It is also important to note that information obtained from *T. foetus* is also valid for *Trichomonas vaginalis*, the agent of human trichomoniasis.

In addition to its importance in veterinary medicine, *T. foetus* (Fig. 1) is also a good representative of one the earliest eukaryotic cells available for study; besides the organelles found in all eukaryotic cells, it contains others such as the hydrogenosomes and a complex and elaborate cytoskeleton, which constitutes the mastigont system (Benchimol, 2004, 2010; Honigberg et al., 1971). The mastigont system (Fig. S1) comprises a well-organized array of microtubules, known as the pelta-axostylar complex, which constitutes an axial skeleton formed by stable, longitudinally oriented microtubules and extends across the length of the cell. The pelta is a structure that supports the flagellar canal from which the flagella emerges (Honigberg et al., 1971; Benchimol, 2004), whereas the axostyle promotes the axial support of the cells and it also participates in karyokinesis during the cell division in *T. foetus* (Ribeiro and Monteiro-Leal, 2000). In addition, there are filaments and lamellae that are not well characterized, such as the supra- and infra-kinetosomal bodies, sigmoidal filaments and the comb (Viscogliosi and Brugerolle, 1994). *T. foetus* possesses a large striated root fibril found only in trichomonads that has an undulating membrane, known as a costa that is thought to provide mechanical support to this structure. Other striated fibers present in this protist are the parabasal filaments, which are thinner than the costa and connect the basal bodies to the first Golgi cisternae, possibly to support this organelle (Benchimol et al., 1993; Benchimol et al., 2001).

The structural organization of the cytoskeleton of trichomonads has been analyzed using several techniques, such as immunofluorescence microscopy using several antibodies (Batista et al., 1988; Benchimol and de Souza, 1987; Viscogliosi and Brugerolle, 1993), high-voltage electron microscopy of whole cells (Benchimol and de Souza, 1987) and transmission electron microscopy using the following methods: (a) thin sections (Batista et al., 1988;

* Corresponding author. Address: Rua Jornalista Orlando Dantas 59, Botafogo, CEP 22231-010 Rio de Janeiro, RJ, Brazil.
E-mail address: marlenebenchimol@gmail.com (M. Benchimol).

1047-8477/$ - see front matter © 2013 Elsevier Inc. All rights reserved.
http://dx.doi.org/10.1016/j.jsb.2013.07.002

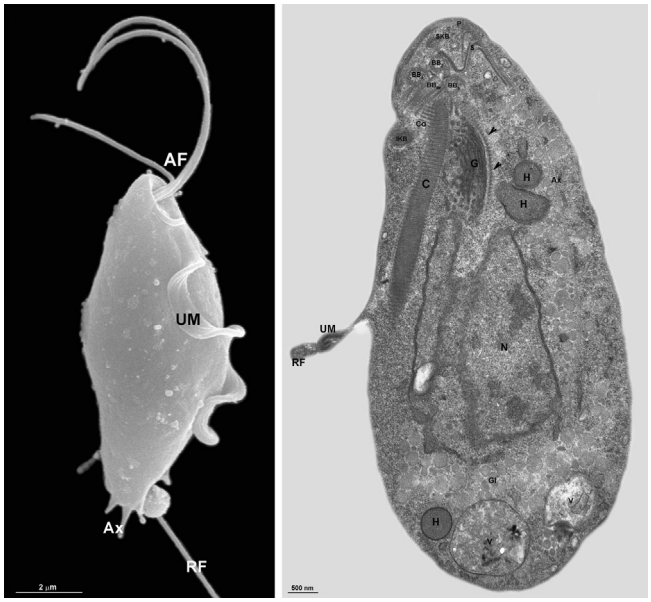

Fig.1. A general view of *T. foetus* by SEM (a) and TEM (b). Note that the parasite displays three anterior flagella (AF), one recurrent flagellum (RF) forming the undulating membrane (UM), the pelta (P), which supports the flagellar canal, and the axostyle (Ax). Nucleus (N), sigmoid filaments (S), supra-kinetosomal body (SKB), basal bodies (BB1–3), basal body of the recurrent flagellum (BBr), costa (C), infrakinetosomal body (IKB), comb (Co), hydrogenosomes (H), Golgi complex (G), parabasal filaments (arrowheads), glycogen (Gl), vacuoles (V). Bars, (a) 2 µm and (b) 500 nm.

Benchimol and de Souza, 1987; Granger et al., 2000; Ribeiro and Monteiro-Leal, 2000), (b) negative staining, (c) freeze-fracture and freeze-etching (Benchimol et al., 1993, 1996, 2000). Important information was obtained with all of these techniques, and we currently have a good understanding of the trichomonad cytoskeleton. However, our previous experience with other protozoa has shown that the use of new high resolution microscopy may yield additional information, even when the structure of a cell type has previously been examined in detail with the available techniques. In recent years, there have been significant advances with scanning electron microscopes. Indeed, new microscopes can reach a resolution in the range of 0.8 nm even using low voltages and samples coated only with a very thin metal or carbon layer. The use of such equipment has revealed new details on the three-dimensional organization of some biological structures. In this paper, we describe new observations of the cytoskeleton of *T. foetus* using high resolution scanning electron microscopy.

2. Materials and methods

2.1. Cells culture

The K strain of *T. foetus* was isolated by Dr. H. Guida (Embrapa, Rio de Janeiro, Brazil) from the urogenital tract of a bull, and it has been maintained in culture for several years. Cells were cultivated in TYM Diamonds medium (Diamond, 1957) supplemented with 10% fetal calf serum. The cells were grown for 24 h at 36.5 °C.

2.2. Cytoskeleton extraction

A 10 µl drop of 0.01% poly-L-lysine (mol wt 150,000–300,000, Sigma, USA) was placed on glass coverslip, allowing to stand for at least 15 min. Afterwards, the coverslips were rinsed in distilled water and a 20 µl drop of the living cells (1×10^7 cells/ml) was placed over the coverslip for 15 min. Samples were rinsed in phosphate-buffered saline (PBS), pH 7.2, to remove cells that did not adhere. For cytoskeleton extraction cells were treated with 2% Triton X-100 and 2% NP-40 in a modified buffer special for isolation of the cytoskeleton (IC buffer −10 mM Tris Base, 2 mM EDTA, 2 mM DTT, 2 mM $MgSO_4$, 150 mM KCl, 30% glycerol, pH 7.4) for 30 min or 1 h (Palm et al., 2005).

2.3. Scanning electron microscopy

For SEM, the IC buffer was removed and the whole *T. foetus* cytoskeleton was fixed in 2.5% glutaraldehyde in 0.1 M phosphate buffer, pH 7.2, washed in PBS, pH 7.2 and then post-fixed for 30 min in 1% OsO_4 in 0.1 M phosphate buffer, pH 7.2, dehydrated in an ascending series of ethanol ending in 100% ethanol, critical point dried with CO_2 using a Bal-Tec CPD 030 critical point drier, and sputter-coated with a thin layer (1–2 nm) of chromium or carbon using a Leica EM SCD 500 or 005 sputter coater. The Nova NanoLab 600 (FEI Company, The Netherlands) scanning electron microscope and Magellan (Extreme High Resolution Scanning Electron Microscope – XHR-SEM) scanning electron microscope (FEI Company, The Netherlands) was used operating at an accelerating voltage of 2 and 1 kV, respectively. For a better identification of some structures, colors were added to some images using Adobe Photoshop color balance.

3. Results and discussion

In previous papers, we have used conventional scanning electron microscopy to analyze the structural organization of *T. foetus* (Benchimol, 2004, 2005). The images obtained allowed a clear characterization of the general shape of the protozoan and, when the inner portion of the cell was exposed due to detergent extraction, to identify components of the cell such as the nucleus, the pelta-axostylar system and the costa. We decided to re-analyze the structural organization of the protozoan using an ultra-high resolution scanning electron microscope due to results obtained with this technique in other protozoa, such as *Toxoplasma gondii* and *Giardia lamblia*, where it was possible to observe new cytoskeleton structures (SańAnna et al., 2005; Maia et al., 2013; Travassos et al., in preparation). For this analysis, we used a scanning electron microscopes where a resolution of 0.8 nm can be attained. Although very low beam landing energies was demonstrated more than 20 years ago, keeping a nanometric spot size below 1 keV, only recently the first commercial SEM succeed in delivering sub-nanometer resolution at 1 kV, but still with some restrictions. Recently, the introduction of the extreme high resolution SEM has demonstrated sub-nanometer resolution in the entire 1–30 kV range (Roussel et al., 2009). Thus, images with elaborate details of the exposed surface could be acquired due some factors: (1) the use of the modified IC buffer allowed a better preservation of the cytoskeleton of *T. foetus* during the membrane extraction procedure; (2) the light coat with 1 to 2 nm thick film of chromium, which has a grain size of 0.3–0.5 nm (Apkarian et al., 1990) or carbon to avoid coating of some delicate structures and (3) an scanning mode that reduces the effects of chromatic aberrations at lower energies (1–2 kV) and minimizes the appearance of image artifacts (Roussel et al., 2009). The use of these technical procedures allowed the observation of the thin filaments that were only observed previously in replicas of quick-frozen, freeze-fractured and deep-etched cells (Benchimol et al., 1996). Some modifications were performed on IC buffer to improve the exposure of the *T. foetus* cytoskeleton. The addition of glycerol to IC buffer prevented the aggregation of particulate cytoplasmic constituents and depolymerization of tubulin (Larson and Dingle, 1981). The preservation of the cytoskeleton structures using the similar buffers as mentioned above have also been demonstrated in different protists

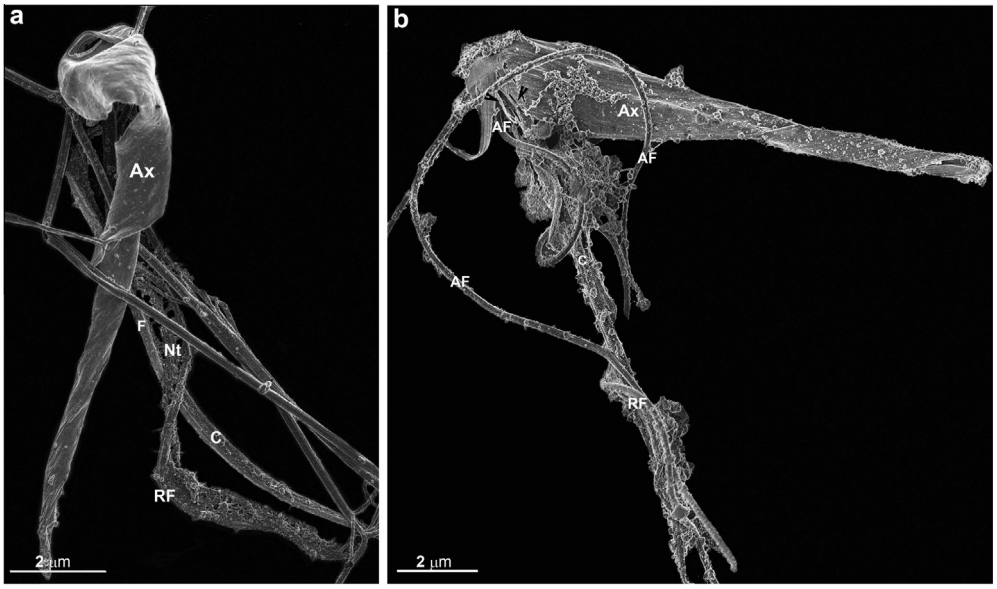

Fig.2. *T. foetus* after detergent extraction as observed by nano-SEM (a) and XHR-SEM (b). The stable structures of the cytoskeleton are more clearly visualized than with routine SEM. Microtubular structures such as the pelta (P) are found in the anterior region of the cell, followed by the axostyle (Ax), which twists at its end portion. The costa (C) exhibits an accessory filament (F), which is connected to the recurrent flagellum (RF) by a filamentous network (Nt). Using XHR-SEM (b), the sigmoid filaments (arrowheads) are more clearly seen. Bars: 2 μM.

(Larson and Dingle, 1981; Lechtreck and Melkonian, 1991; Lechtreck et al., 1996; Palm et al., 2009).

3.1. Pelta-axostylar system

Although the pelta-axostyle system is a structure that is easily observed by conventional SEM after plasma membrane removal, in most cases it is visualized as totally smooth or with smooth grooves (Benchimol, 2005). Using high-resolution SEM, details that were not previously seen with SEM were observed. The axostyle (Fig. 2, Ax) appeared as a sheet of microtubules that forms a hollow tube, which is opened on the anterior region forming a spoon-like area known as a capitulum. The pelta was visualized as a crescent ribbon of the microtubules on the internal face of the capitulum, which extends to apically surround the walls of the periflagellar canal. The images obtained allowed us to clearly resolve the micro-

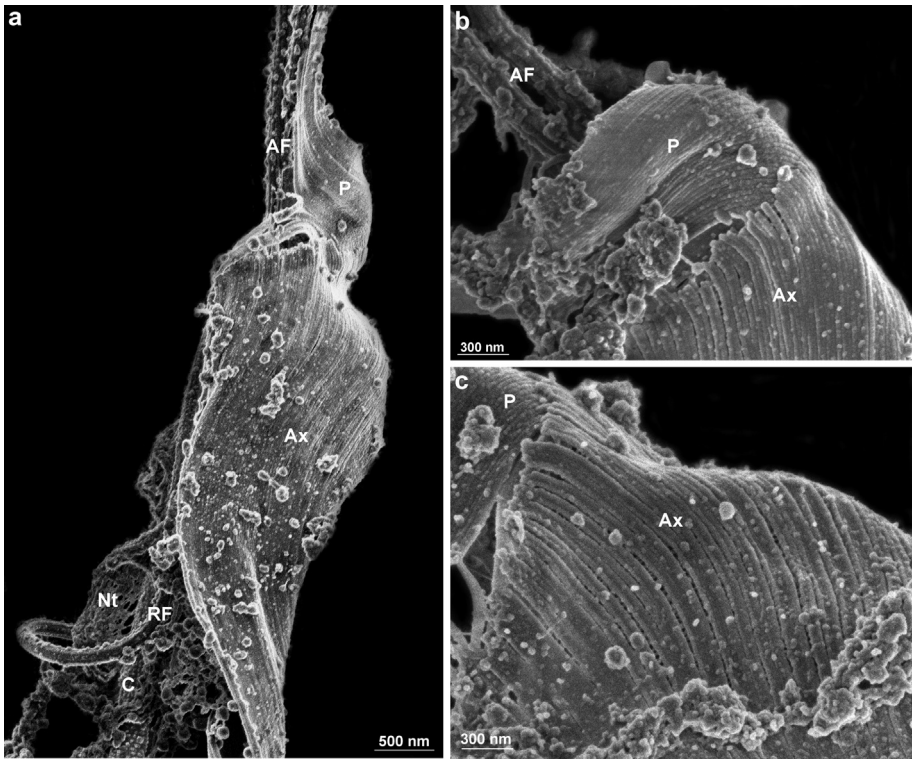

Fig.3. XHR-SEM of the pelta-axostylar system. (a) An overview of the pelta (P) that is located in the anterior region, supporting the flagellar canal and the axostyle (Ax). (b–c) Inset of the pelta-axostyle junction. Note that each microtubule is clearly visualized and that they are organized in two distinct groups. Bars: (a) 500 nm; (b–c) 300 nm.

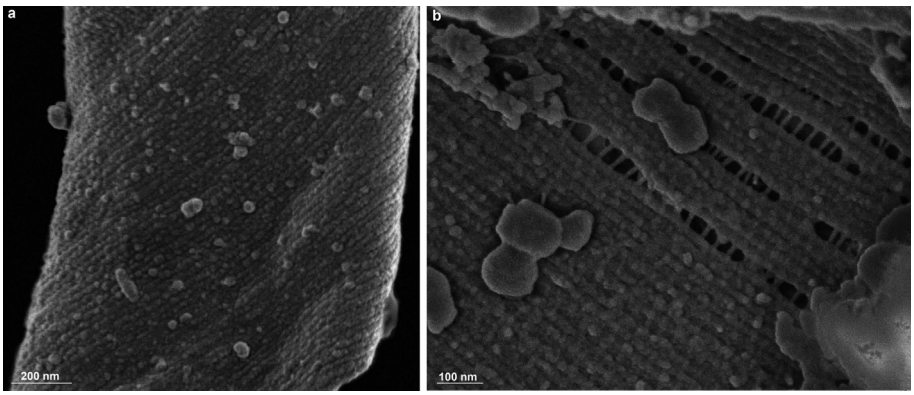

Fig.4. XHR-SEM of the *T. foetus* axostyle, where the microtubules can be seen clearly (a). (b) At higher magnification, the bridges connecting the axostyle (Ax) microtubules are more clearly seen, and these bridges had a thickness of 10.4 nm ± 1.0. Bars: (a) 200 nm and (b) 100 nm.

tubules forming a sheet that twists at its end portion (Figs. 3 and 4). Furthermore, the extremities of these microtubules were seen for the first time. We could also see that the microtubules of the pelta (P) and the axostyle (Ax) were easily distinguished as two groups (Fig. 3b–c) with different orientations. Although these structures act together to promote the cell support, it is possible that these structures may also have independent motion and functions. The pelta-axostylar junction was clearly observed for the first time. Previous studies using either TEM of thin sections or quick-freezing and freeze-etching of trichomonads have shown that axostyles are not only composed of adjacent microtubules but also connected to each other by filamentous bridges (Benchimol et al., 1993; Benchimol et al., 2000; Mooseker and Tilney, 1973). These bridges could be clearly identified by XHR-SEM; they had a thickness of 10.4 ± 1.0 nm and were spaced at intervals ranging from 9 nm to 25.4 nm (Fig. 4). Similar bridges that link microtubules of the contractile axostyles were also described in protozoa of the hingut of the *Cryptocercus* (Mooseker and Tilney, 1973). In these protozoa the bridges are composed by a single subunit of the dinein and its function is related with motion generation by interactions between adjacent rows of microtubules (Mooseker and Tilney, 1973). However, further biochemical studies in *T. foetus* are necessary to better describe the protein composition and function of these bridges.

3.2. Costa and accessory structure

Although previous reports have suggested that the costa of *T. foetus* is predominantly composed of carbohydrates (Lemoine et al., 1983; Sledge et al., 1978), cytochemical (Benchimol et al., 1982) and biochemical studies carried out in *T. foetus* (Monteiro-Leal et al., 1993) and other trichomonads (Amos, 1979; Goodwin and Samuels, 1971, 1972; Viscogliosi and Brugerolle, 1993) clearly showed that this structure is mainly composed of proteins. Its function is related to mechanical support for the undulating membrane, because the costa is found only in trichomonads that possess this structure (Honingberg et al., 1971). Our present observations show that the costa may reach a length of 14.38 ± 1.3 μm and is 36.5 ± 3.4 nm wide with alternating bands 13.8 + 1.25 nm and 241.3 ± 13.9 nm in width.

More importantly, a new accessory was observed running along the right-hand side of the costa (Figs. 2a, 5–7, C). Similarly the costa, the accessory filament forms a striated pattern, but these structures are originated in sites with opposite directions (Fig. 5, ★). To the best of our knowledge, this report is the first description of this structure. Honigberg et al., 1971 described a filament that branched off the costa, and we have shown previously, in replicas of quick-frozen, freeze-fractured, deep-etched and rotary-replicated cells, the presence of pits at the periphery of the costa (Benchimol, 1993). Transmission electron microscopy of thin sections also revealed the presence of a structure that may correspond to the costa accessory filament (Benchimol, 2010). However, a 3-D view of the structure was achieved with high-resolution SEM. The accessory filament could help the costa to support the beat of the undulating membrane. However, additional studies are necessary to confirm this hypothesis.

Previous studies using replicas from quick-frozen, freeze-fractured, deep-etched and rotary-replicated cells revealed that the

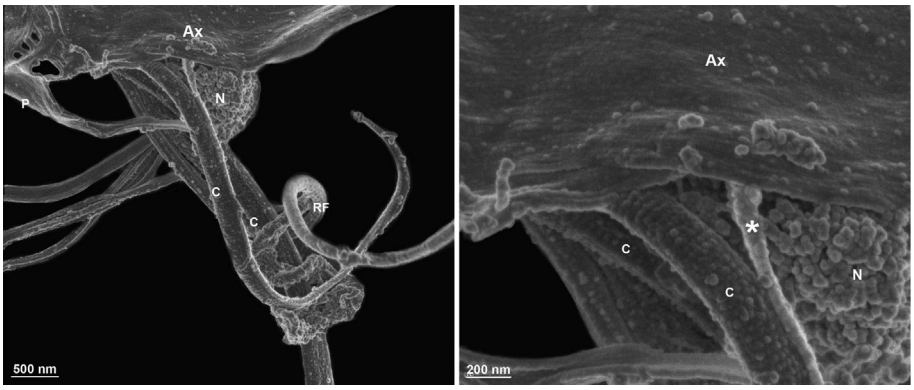

Fig.5. Nova Nano-SEM images of the cytoskeleton of the *T. foetus*, where two costa (C) are seen, indicating that the cell is dividing. Note the presence of an accessory fifilament (∗), which is originated in the anterior cell region, separately from the costa; these structures are joined together at the anterior cell region and remain associated throughout their length. Both structures have a periodic pattern. Other structures such as the pelta (P), axostyle (Ax), recurrent flagellum and nucleus were also observed. Bars: (a) 50 nm and (b) 200 nm.

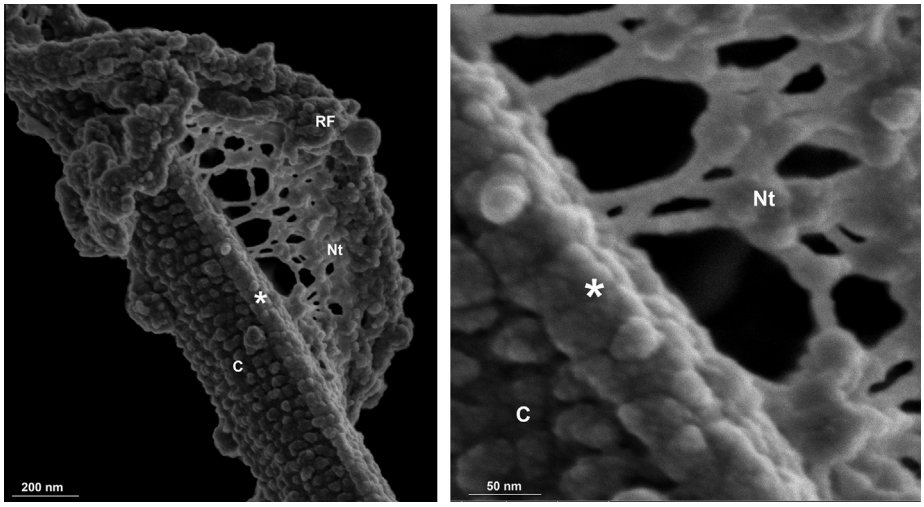

Fig.6. XHR-SEM of the filamentous network (Nt) located under the undulating membrane, which connects the accessory filament (★) of the costa (C) to the recurrent flagellum (RF) (a). At higher magnification, it is possible to observe that this network is made of filamentous and globular structures (b). Bars: (a) 200 nm and 50 nm.

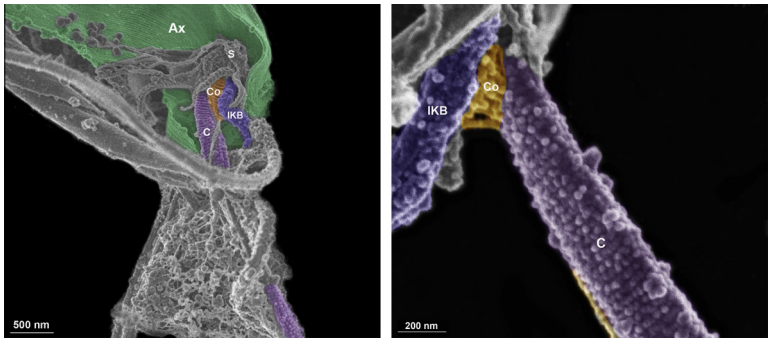

Fig.7. XHR-SEM of *T. foetus* anterior region. Notice the details of some cytoskeletal structures along with their interactions, such as the microtubules of the axostyle (Ax) (a), the comb (Co), seen as a scalariform structure that is composed of small filaments (a–b) connecting the costa (C), and the infra-kinetosomal body (IKB). The sigmoidal filaments (S) are found over the basal bodies. Bars: (a) 500 nm and (b) 200 nm.

recurrent flagellum establishes a specialized junction with a surface projection of the cell body where a large number of filaments emerge from pits in the costa and make contact with a network of other filaments (Benchimol et al., 1993; Monteiro Leal et al., 1993). The presence of a filamentous network connecting the costa to the undulating membrane supports the view that the costa aids in controlling the mechanical pressure released during recurrent flagellum beating (Benchimol et al., 1993). However, other electron microscopy techniques did not confirm the presence of such a filamentous network. Now, using high-resolution SEM, this network was easily observed; it is composed of 12.5 ± 1.2 nm thick filaments, which may reach a length of 73.6 ± 9.1 nm, and of globular structures with a mean diameter of 29.20 ± 3.3 nm (Fig. 6, Nt). Further biochemical studies are necessary to identify the nature of the proteins which make the filamentous network. We also observed that the costa interacted with other cytoskeletal structures, such as the comb (Fig. 7, Co), which connects the costa to the infrakinetosomal body and has been described as a scalariform structure found in *T. foetus,* but not in *Trichomonas vaginalis* (Benchimol, 2010; Viscogliosi and Brugerolle, 1993). In the present study, the comb appeared to be formed by small filaments that were perpendicularly oriented in relation to the costa (Fig. 7b).

3.3. Other filaments

High-resolution SEM also allowed clear observation of the parabasal filaments (Fig. 8, PF), which are striated structures that have been implicated in the support of the large Golgi complex of trichomonads and may reach a length of 5 μm (Benchimol, unpublished). The *T. foetus* parabasal filaments were seen as striated fibers that were thinner (128.5 ± 9.6 nm) and shorter than the costa, although their periodicity (40.2 ± 5.4 nm) was rather similar to the costa. Interestingly, both the parabasal filaments and costa were observed to be connected to a network of 12.2 ± 2.5 nm thick cytoskeleton filaments (Fig. 8), as well as to the nucleus (data not shown). This connection may explain the anterior position of the nucleus, which is always localized near the axostyle. Previous studies have shown that *T. foetus* has two parabasal filaments, whereas *T. vaginalis* has three of these filaments (Lee et al., 2009).

We were also able to visualize the sigmoidal filaments, which are sigma-shaped striated roots that were previously observed by conventional TEM in the anterior region of *T. foetus* (Viscogliosi and Brugerolle, 1993). Although these filaments have been labeled, as seen by fluorescence microscopy, with antibodies recognizing the protein centrin, their function is presently unknown. Our observations showed that the sigmoidal filaments appear to be formed of at least six filaments, which are located near the pelta and the axostyle (Fig. 7). Interestingly, for the first time, striations with a periodicity of 50.5 ± 6.6 nm could be detected in this structure. Previous descriptions of the SF indicated the presence of eight or nine sigmoid filaments (Honigberg et al., 1971) that extended between basal body #2 and terminated at the inner surface of the pelta-axostylar junction (Benchimol et al., 2000; Viscogliosi and Brugerolle, 1993). Honigberg et al. (1971) reported that this

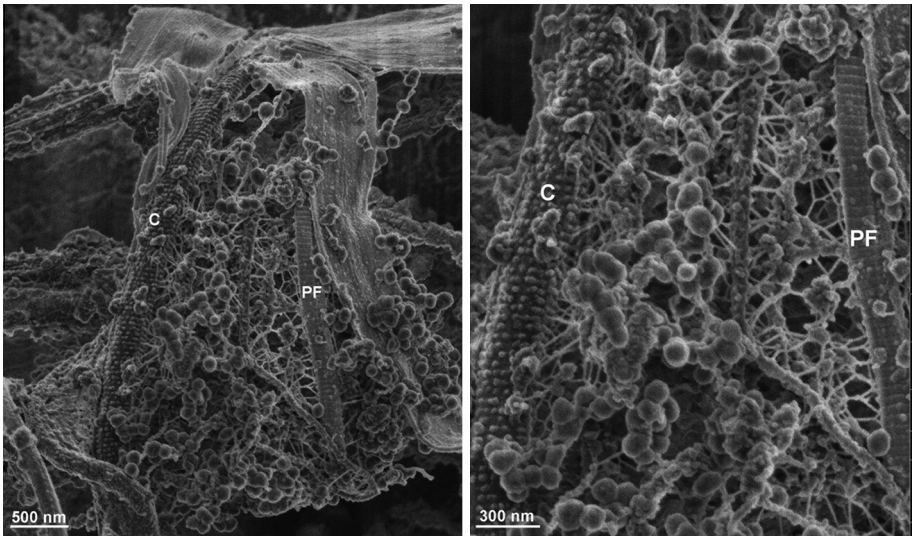

Fig.8. XHR-SEM of the striated fibers of *T. foetus*. The costa (C) is seen as the thickest fiber, while the parabasal filament (PF) is slightly flattened. Both structures have similar periodicity. Note the network formed by the filamentous structures, which are well-preserved with this approach and support these structures. Bars: (a) 500 nm and (b) 300 nm.

association occurs through proteinaceous bridges, which were not observed in our preparations.

In conclusion, our observations of the cytoskeleton of *T. foetus* using high-resolution SEM not only confirmed previous studies but also allowed a better understanding of the three-dimensional structural organization of this important pathogenic protozoan. In addition, this approach revealed the presence of new structures, such as the costa accessory filament, and the presence of two groups of microtubules that form the pelta-axostylar system. Taken together, these results may contribute in future studies concerning the functional analysis of cytoskeletal structures of trichomonads.

Acknowledgments

This work was supported by the Conselho Nacional de Desenvolvimento Científico e Tecnológico (CNPq), the Coordenação de Aperfeiçoamento de Pessoal de Nível Superior (CAPES), the Fundação Carlos Chagas Filho de Amparo à Pesquisa do Estado do Rio de Janeiro (FAPERJ), the Programa de Núcleos de Excelência (PRONEX), the Financiadora de Estudos e Projetos (FINEP), and the Instituto Nacional de Metrologia, Qualidade e Tecnologia (Inmetro). The authors thank Luis Sérgio de Araújo Cordeiro Júnior for technical support.

Appendix A. Supplementary data

Supplementary data associated with this article can be found, in the online version, at http://dx.doi.org/10.1016/j.jsb.2013.07.002.

References

Amos, W.B., Grimstone, A.V., Rotshild, L.J., Allen, R.D., 1979. Structure, protein composition and birefringence of the costa: a motile flagellar root fibre in the flagellate *Trichomonas*. J. Cell Sci. 35, 139–164.

Apkarian, R.P., Gutekunst, M.I., Joy, D.C., 1990. High resolution SEM study of enamel crystal morphology. Electron Microsc. Tech. 14, 70–78.

Batista, C.M., Benchimol, M., Cunha e Silva, N.L., de Souza, W., 1988. Localization of acetylated alpha-tubulin in *Tritrichomonas foetus* and *Trichomonas vaginalis*. Cell Struct. Funct. 13, 445–453.

Benchimol, M., 2004. Trichomonads under microscopy. Microsc. Microanal. 10, 528–550.

Benchimol, M., 2005. New ultrastructural observations on the skeletal matrix of *Tritrichomonas foetus*. Parasitol. Res. 97, 408–416.

Benchimol, M., 2010. The mastigont system. In: de Souza, Wanderley (Ed.), Structures and Organelles in Pathogenic Protists, . first ed., vol. 1 London, Springer-Verlag, pp. 1–26.

Benchimol, M., de Souza, W., 1987. Structural analysis of the cytoskeleton of *Tritrichomonas foetus*. J. Submicrosc. Cytol. 19, 139–147.

Benchimol, M., Elias, C.A., de Souza, W., 1982. *Tritrichomonas foetus*: ultrastructural localization of basic proteins and carbohydrates. Exp. Parasitol. 54, 135–144.

Benchimol, M., Kachar, B., de Souza, W., 1993. The structural organization of the pathogenic protozoan Tritrichomonas foetus as seen in replicas of quick frozen, freeze-fractured and deep etched cells. Biol. Cell. 77, 289–295.

Benchimol, M., Kachar, B., de Souza, W., 1996. The structural organization of the pathogenic protozoan *Tritrichomonas foetus* as seen in replicas of quick frozen, freeze-fractured and deep etched cells. Biol. Cell. 77, 289–295.

Benchimol, M., Diniz, J.A., Ribeiro, K., 2000. The fine structure of the axostyle and its associations with organelles in Trichomonads. Tissue Cell. 32, 178–187.

Benchimol, M., Ribeiro, K.C., Mariante, R.M., Alderete, J.F., 2001. Structure and division of the Golgi complex in *Trichomonas vaginalis* and *Tritrichomonas foetus*. Eur. J. Cell Biol. 80, 593–607.

Diamond, L.S., 1957. The establishment of various trichomonads of animals and man in axenic cultures. J. Parasitol. 43, 448–490.

Goodwin, F.L., Samuels, R., 1971. Isolation and characterization of costa in Tritrichomonas augusta. J. Protozool. 18 (Suppl.), 16.

Goodwin, F.L., Samuels, R., 1972. Sodium dodecyl sulfate polyacrilamide gel electrophoresis of tritrichomonads costa protein. J. Protozool. 19 (Suppl.), 31.

Gookin, J.L., Stebbins, M.E., Hunt, E., Burlone, K., Fulton, M., et al., 2004. Prevalence of and risk factors for feline *Tritrichomonas foetus* and giardia infection. J. Clin. Microbiol. 42, 2707–2710.

Granger, B.L., Warwood, S.J., Benchimol, M., De Souza, W., 2000. Transient invagination of flagella by *Tritrichomonas foetus*. Parasitol. Res. 86, 699–709.

Honigberg, B.M., Mattern, C.F., Daniel, W.A., 1971. Fine structure of the mastigont system in *Tritrichomonas foetus* (Riedmüller). J. Protozool. 18, 183–198.

Larson, D.E., Dingle, A.D., 1981. Isolation, ultrastructure, and protein composition of the flagellar rootlet of *Naegleria gruberi*. J. Cell Biol. 89, 424–432.

Lechtreck, K.F., Melkonian, M., 1991. Striated microtubule-associated fibers: identification of assemblin, a novel 34-kD protein that forms paracrystals of 2-nm filaments in vitro. J. Cell Biol. 115, 705–716.

Lechtreck, K.F., Frins, S., Bilski, J., Teltenkötter, A., Weber, K., Melkonian, M., 1996. The cruciated microtubule-associated fibers of the green alga *Dunaliella bioculata* consist of a 31 kDa SF-assemblin. J. Cell Sci. 109, 827–835.

Lee, K.E., Kim, J.H., Jung, M.K., Arii, T., Ryu, J.S., Han, S.S., 2009. Three-dimensional structure of the cytoskeleton in Trichomonas vaginalis revealed new features. J. Electron Microsc. 58, 305–313.

LeMoine, L.A., Hart, L.T., Larson, A.D., McCorkle-Shirley, S., 1983. Costa as a glycogen store and probable site of energy generation in *Tritrichomonas foetus*. Am. J. Vet. Res. 44, 713–714.

Monteiro-Leal, L.H., da Cunha-e-Silva, N.L., Benchimol, M., de Souza, W., 1993. Isolation and biochemical characterization of the costa of *Tritrichomonas foetus*. Eur. J. Cell Biol. 60, 235–242.

Mooseker, M.S., Tilney, L.G., 1973. Isolation and reactivation of the axostyle. Evidence for a dynein-like ATPase in the axostyle. J. Cell Biol. 56, 13–26.

Palm, D., Weiland, M., McArthur, A.G., Winiecka-Krusnell, J., Cipriano, M.J., Birkeland, S.R., Pacocha, S.E., Davids, B., Gillin, F., Linder, E., Svärd, S., 2005. Developmental changes in the adhesive disk during *Giardia* differentiation. Mol. Biochem. Parasitol. 141, 199–207.

Rae, D.O., Crews, J.E., 2006. Tritrichomonas foetus. Vet. Clin. North Am. Food. Anim. Pract. 22, 595–611.
Ribeiro, K.C., Monteiro-Leal, L.H., Benchimol, M., 2000. Contributions of the axostyle and flagella to closed mitosis in the protists *Tritrichomonas foetus* and *Trichomonas vaginalis*. J. Eukaryot. Microbiol. 47, 481–492.
Roussel, L.Y., Stokes, D.J., Gestmann, I., Darus, M., Young, R.J., 2009. Extreme high resolution scanning electron microscopy (XHR SEM) and beyond. Proc. of SPIE 7378, 73780W–73789W.
Sant'Anna, C., Campanati, L., Gadelha, C., Lourenço, D., Labati-Terra, 2005. Improvement on the visualization of cytoskeletal structures of protozoan parasites using high-resolution field emission scanning electron microscopy (FESEM). Histochem. Cell Biol. 124, 87–95.
Sledge, W.E., Larson, A.D., Hart, L.T., 1978. Costae of *Tritrichomonas foetus*: purification and chemical composition. Science 199, 186–188.
Stockdale, H.D., Givens, M.D., Dykstra, C.C., Blagburn, B.L., 2009. *Tritrichomonas foetus* infections in surveyed pet cats. Vet. Parasitol. 160, 13–17.
Viscogliosi, E., Brugerolle, G., 1993. Cytoskeleton in trichomonads: I. Immunological and biochemical comparative study of costal proteins in the genus Tritrichomonas. Eur. J. Protistol. 29, 160–170.
Viscogliosi, E., Brugerolle, G., 1994. Striated fibers in trichomonads: costa proteins represent a new class of proteins forming striated roots. Cell Motil. Cytoskeleton 29, 82–93.
Yaeger, M.J., Gookin, J.L., 2005. Histologic features associated with *Tritrichomonas foetus*-induced colitis in domestic cats. Vet. Pathol. 42, 797–804.